Journal of King Saud University – Science 35 (2023) 102509

Contents lists available at ScienceDirect

Journal of King Saud University – Science

journal homepage: www.sciencedirect.com

Original article

Contamination and health risk assessment of surface sediments along Ras Abu Ali Island, Saudi Arabia

Khaled Al-Kahtany, Abdelbaset S. El-Sorogy *

Geology and Geophysics Department, College of Science, King Saud University, Saudi Arabia

ARTICLE INFO

Article history:
Received 23 July 2022
Revised 29 November 2022
Accepted 12 December 2022
Available online 15 December 2022

Keywords:
Heavy metals
Coastal sediment
Human risk
Chronic daily intake
Arabia Gulf

ABSTRACT

The coastline of the Arabian Gulf attracts people throughout the year for tourism and fishing activities. The present work aimed to document the contamination and human health assessment of heavy metals (HMs) in 34 surface sediment samples collected along Ras Abu Ali coastline, Saudi Arabia. Enrichment factor (EF), contamination factor (CF), and sediment quality guideline (SQG) were calculated to estimate the sediment contamination, while the hazard index (HI), cancer risk (CR), and total lifetime cancer risk (LCR) were determined for human health assessment via ingestion and dermal contact pathways on both adults and children. The averages of the HMs (μg/g dry weight) were in the following order: Fe (4808) > Ni (13.00) > Zn (6.89) > Cr (7.86) > V (6.67) > Cu (4.14) > Pb (3.50) > As (2.47) > Co (1.43). Results of EF indicated minor enrichment with Ni, Pb, and As, and no enrichment with the remaining HMs. Based on CF, the coastal sediments of Ras Abu Ali showed low contamination with HMs. Reported values of As, Cr, Cu, Pb, and Zn were lower than the ISQG-Low values, however, 4 samples of Ni reported values between the ISQG-Low and ISQG-High values, indicating some anthropogenic effects with Ni. HI values were higher among children in comparison to adults, suggesting that children were at higher risk of non-carcinogenic exposure than adults. LCR values indicated that no significant health hazards for people inhabited the study area from the carcinogenic Pb, Cr, and As.

1. Introduction

Contamination of coastal sediment is widely recognized as a severe environmental issue, and it is critical to examine the ecological and health consequences of HMs in coastal sediment. The historical development of industrialized and residential complexes on coastal zones around the world represents a strong pressure on the capacity of natural systems and human health to assimilate the high amount of waste derived from human activities (Bellas et al., 2020; Di Cesare et al., 2020; Tonne et al., 2021; Saavedra and Quiroga, 2021). HMs discharged into aquatic environments will be accumulated in marine sediments causing an ecological risk to filter-feeder organisms, and ultimately affecting humans (El-Sorogy and Youssef, 2015; Singovszka et al., 2017; Ustaoğlu and Tepe, 2019; Rajeshkumar et al., 2018; Wu et al., 2014).

HMs enter the human body through inhalation from air, sediment/dust ingestion, and skin contact (Naveedullah Hashmi et al., 2014; Nazzal et al., 2021). Excessive HM intake in the human body can cause neurological, cardiovascular, and chronic kidney diseases, tumors, and even cancers (Song and Li, 2014; Pan et al., 2018). Children are particularly sensitive to HMs because they experience additional routes of exposure from breastfeeding, placental exposure, hand-to-mouth activities in early years, and lower toxin elimination rates (Ma et al., 2016; Rahman et al., 2021).

During the last two decades, the coastal sediments along the eastern and western sides of the Arabian Gulf have been subjected to intensive environmental studies (e.g., El-Sorogy et al., 2019, 2018a; Alharbi et al., 2017; Al-Kahtany et al., 2018). These studies evaluated the HM contamination using different pollution indices and background references. Studies on human health assessment using hazard index, and total lifetime cancer risk via ingestion and dermal contact on both adults and children are still scares. Therefore, the objectives of the present work are: (i) to determine the levels and document the distribution of V, Fe, As, Co, Ni, Zn, Cr, Pb, and Cu in marine sediments along Abu Ali Island, Saudi Arabia,

* Corresponding author at: Department of Geology and Geophysics, College of Science, King Saud University, P.O. box 2455, Riyadh 11451, Saudi Arabia.
E-mail address: asmohamed@ksu.edu.sa (A.S. El-Sorogy).

Peer review under responsibility of King Saud University.

Production and hosting by Elsevier

https://doi.org/10.1016/j.jksus.2022.102509
1018-3647/© 2022 The Author(s). Published by Elsevier B.V. on behalf of King Saud University.

(ii) to assess the degree of HM contamination, and (iii) to determine the potential health risks of these HMs as cumulative carcinogenic and non-carcinogenic risks.

2. Material and methods

2.1. Study area

Ras Abu Ali Island is located at Eastern Province, Saudi Arabia (Fig. 1). The island has a unique crescent shape with the outer section facing north. The coastline is mostly sandy-dominated shore, with rocky and mangrove shores in parts. The sandy shores are mostly bounded by seagrass, dominantly of *Halophila uninervis, H. stipulacea* and *H. ovalis*. The mangrove is represented by mono-specific stands of *Avicennia marina* of less than 2 m height (Saderne et al., 2020). Seagrass and mangroves are under threat due to local dredging activities, land reclamation, and marine pollution (Almahasheer, 2018). The rocky shores and their inhabited molluscs were bioeroded by clionid sponges, duraphagous drillers, endolithic bivalves, polychaete annelids, acorn barnacles, and vermetid gastropods like those previously identified from Al-Khobar, Al-Khafji, Jazan, and Duba areas along the Arabian Gulf and Red Sea coasts (El-Sorogy, 2015; El-Sorogy et al., 2018b, 2020, 2021; Demircan et al., 2021).

2.2. Sampling, analytical methods and data analysis

Thirty-four modern surface sediment samples were collected in January, 2021, from the coastal zone of Ras Abu Ali Island (Fig. 1). Samples were stored in plastic bags and placed in an icebox. In the laboratory, samples were dried in air temperature (18–26 °C) for a week after removing sea grass and gravels, then samples subjected to size fractionation using a nest of sieves to obtain the <63 µm fraction for analysis. A prepared sample (0.50 g) is digested with HNO_3- HCl aqua regia for 45 min in a graphite heating block. The resulting solution is diluted to 12.5 mL with deionized water, mixed and analysed. V, Fe, As, Co, Ni, Zn, Cr, Pb, and Cu were analysed using inductively coupled plasma-atomic emission spectrometry (ICP - AES) in ALS Geochemistry Lab, Jeddah branch, Saudi Arabia. The ICP-AES method was validated in terms of linearity, limits of detection (LOD), limits of quantification (LOQ), accuracy and precision. Calibration curves for each element were constructed by plotting the peak area of the optimum emission line to the concentration of the standard solutions or spike solutions for standard addition curves. Calibration curves showed an excellent linearity for all elements.

The enrichment factor (EF) and contamination factor (CF) were used to assess the HM contamination in sediment samples (Kowalska et al., 2018). The National sediment quality guidelines (SQG) of ANZECC/ARMCANZ was applied to predict the adverse effects produced by polluted sediments on benthic aquatic communities (Simpson et al., 2013). The estimation of the health risks via ingestion and dermal contact pathways on both adults and children can be estimated using of the chronic daily intake (CDI), hazard quotients (HQ), hazard index (HI), cancer risk (CR), and total lifetime cancer risk (LCR). These indices are calculated according to the following formulas (Hakanson, 1980; El-Sorogy and Attiah, 2015; Luo et al., 2012; IRIS, 2020; Mondal et al., 2021):

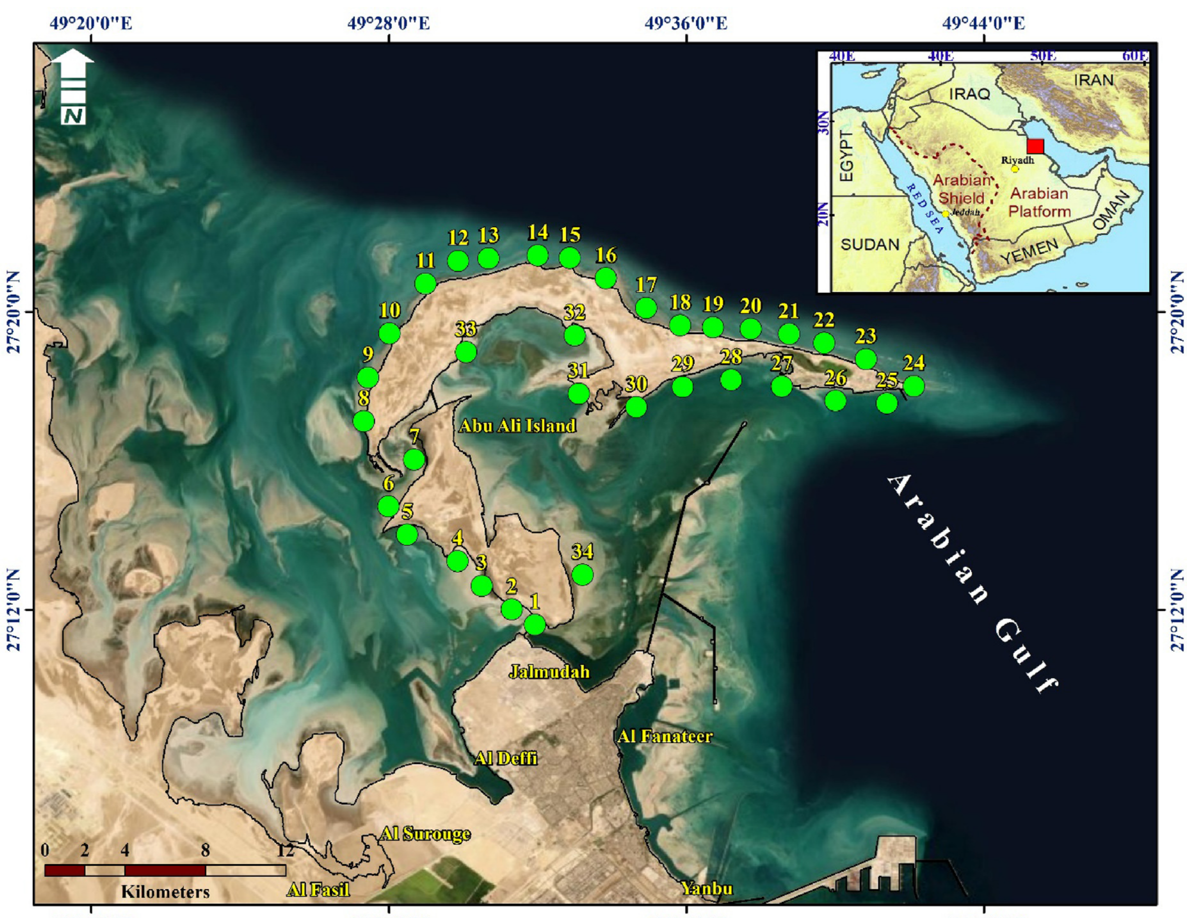

Fig. 1. Location map of the study area and the sampling sites.

$$EF = (M/X)_{sample}/(M/X)_{background}$$

$$CF = C_o/C_b$$

$$CDI_{ingest.} = (Csediment \times IngR \times EF \times ED/BW \times AT) \times CF$$

$$CDI_{dermal} = (Csediment \times SA \times AFsediment \times ABS \times EF \times ED/BW \times AT) \times CF$$

$$HI = \Sigma HQE = HQing + HQdermal$$

$$HQE = CDI/RfD$$

$$Cancer\ \ Risk\ \ (CR) = CDI \times CSF$$

$$LCR = \Sigma Cancer\ \ Risk = CRing + CRdermal$$

Fig. 2. The spatial distribution of As, Co, Pb, Cr, Cu, Ni, V, Zn, and Fe in the study area.

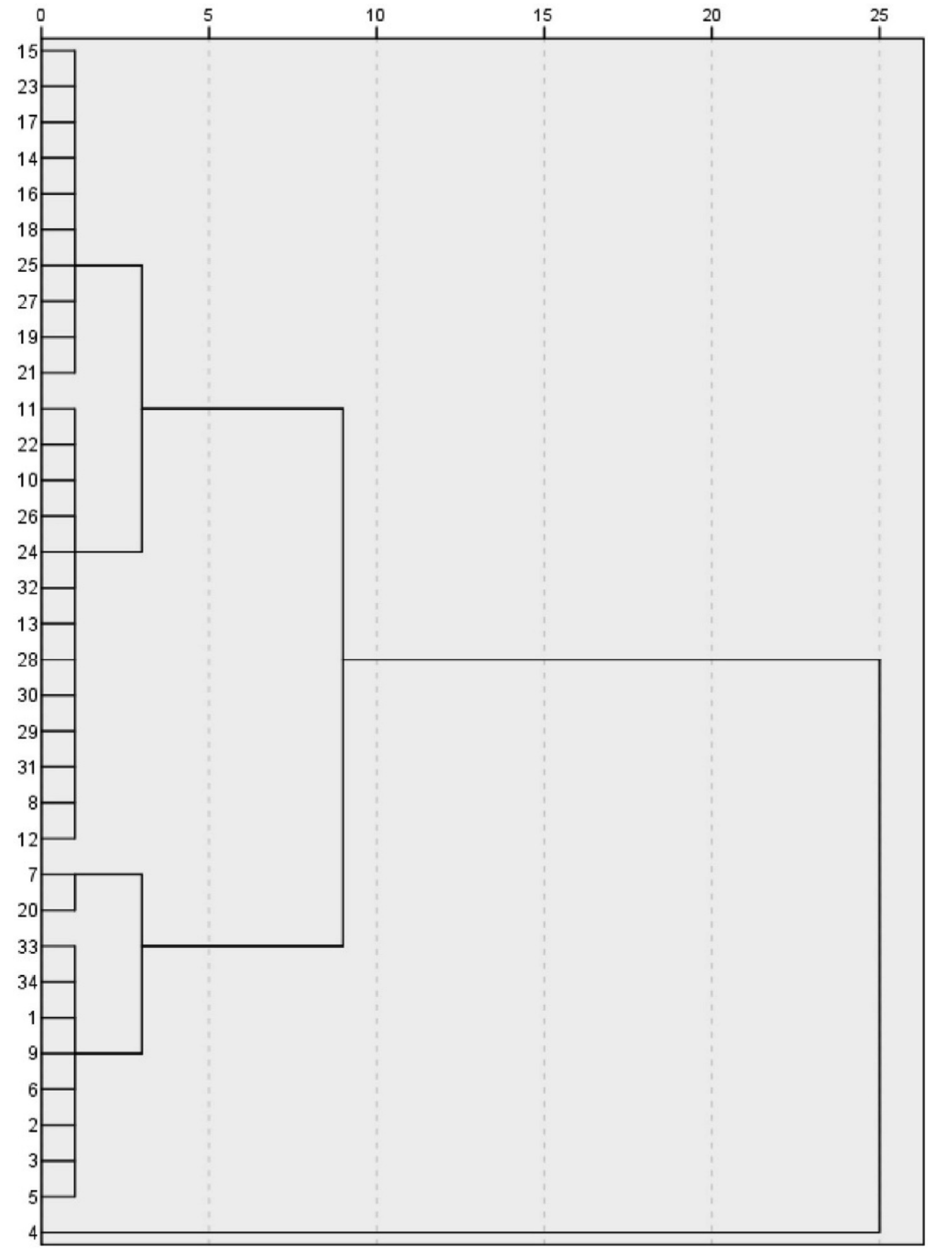

Fig. 3. The Q-mode HCA of the studied sediment samples.

Table 1
The average values of the HMs (µg/g) in the study area with comparison to some worldwide coastal areas, background references and SQGs.

Location and references		As	Co	Cr	Cu	Fe	Ni	Pb	V	Zn
Present study (Ras Abu Ali Island, Saudi Arabia)		2.47	1.43	7.86	4.14	4808	13.00	3.50	6.67	6.89
Gulf of Suez, Egypt (Nour et al., 2022)			7.4	8.98	1.66	540.7	5.58	2.78		3.96
Ordu province, Black Sea, Turkey (Ustaoğlu et al., 2020)			5.13	3.52	13.03	8135	3.62	3.74		25.68
Aqeer coastline, Arabian Gulf (Al-Hashim et al., 2021)		14.99		3.67	11.27	8092	0.57	3.88		7.62
Duba, Red Sea coast, Saudi Arabia (Kahal et al., 2020)			4.13	32.85	31.59	2432	20.03	2.31		28.51
Rosetta, Mediterranean Sea, Egypt (El-Sorogy et al., 2016)		298.22	69.78	0.18	24.57	109,560	480.86	384.68	374.78	183.23
Earth's crust (Yaroshevsky, 2006)		1.7	18	83	47	46,500	58	16	90	83
Continental crust (Rudnick and Gao, 2003)		4.8	17.3	92	28		47	17	97	67
Earth's crust (Turekian and Wedepohl, 1961)		13	19	90	45	47,200	68	20	130	95
Continental crust (Taylor, 1964)		1.8	25	100	55	56,300	75	12.5	135	70
National sediment quality guidelines (Simpson et al., 2013)	ISQG Low	8		80	34		21	50		200
	ISQG high	70		370	270		52	220		410

where M and C_o are the analyzed metal, X and C_b are the level of a normalizer element (Fe), RfD is the reference dose for each HM, and CSF is the carcinogenic slope factor values (mg/kg.day) for Cr, Pb and As (0.5, 0.0085 and 1.5, respectively). The exposure factors used in the estimation of CDI are presented in Supplementary Table 1. Hierarchical cluster analyses (HCA) and Pearson correlation coefficient were performed to identify the potential sources of HMs.

3. Results and discussion

3.1. Concentration and assessment of heavy metals

The coordinates of the selected coastal sediments and the concentrations of HMs (μg/g, dry weight) were presented in Supplementary Table 2. HMs showed the following ranges: Fe (1600–11300), Ni (5.0–31), Zn (1.0–35), Cr (3.0–19), V (2.0–19), Pb (1.0–14), Cu (1.0–11), As (1.0–8), and Co (0.5–4). The highest concentrations of HMs were recorded in S2 (Cu), S4 (Cr and Fe), S6 (As and Ni), S7 (Co, and V), and S20 (Pb and Zn) (Fig. 2). The higher accumulation of HMs in these samples may be attributed to their occurrence in the south western shallow isolated area from the open sea (except S20) and characterized by fine and very fine sized composition (Vieira et al., 2021). In contrast, the samples of the lower HM levels, such as S10, S14, S16, S18, S19, and S21, are characterized by medium to coarse size and occurred in the north of the study area faced to the open sea. The Q-mode HCA subdivided the investigated 34 samples into three clusters (Fig. 3). The first cluster includes S4, which reported the highest values of Cr and Fe. The second cluster accounts 10 samples (S1-S3, S5-S7, S9, S20, S33, and S34), which showed the highest levels of Cu, As, Ni, Co, Pb, Zn, and V. The third cluster contains the remaining 23 samples (S1, S8, S10-S19, and S21-S32), which recorded most of the lowest HM values in the study area.

The average values of the HMs in the sediment samples are listed in Table 1, along with their comparison to background references, SQGs, and some worldwide coastal sediments. Average values of Zn, V, Co, Cu (except Gulf of Suez, Egypt), Fe (except Duba, Red Sea coast, Saudi Arabia) were less than those reported in the worldwide background references, national sediment quality guidelines (when available), and worldwide coastal areas (Table 1). Differently, our average values of Cu, Ni, and Pb were greater than those recorded in the Gulf of Suez, Egypt (Nour et al., 2022). Furthermore, As (2.47 μg/g), was greater than the average earth's crust of Yaroshevsky (2006) and Taylor (1964). As, Cr, Cu, Pb, and Zn exhibited values less than the ISQG-Low values (Simpson et al., 2013), indicating a low risk of these HMs in Ras Abu Ali coastal sediment. However, 4 samples (S4, S6, S7, and S20) reported values of Ni between the ISQG-Low and ISQG-High values, indicating some anthropogenic effects with Ni.

Enrichment factor is used to distinguish between elements contributed by human intervention from those of geological origin (Reimann and de Caritat, 2005; Kahal et al., 2020). Average EF values in the study area indicated minor enrichment with Ni, Pb, and As, and no enrichment with the remaining HMs (Table 2). S19 showed moderately severe enrichment with Ni (EF = 5.64), while S29 and S19 revealed moderate enrichment with As and Pb (EF = 4.64 and 4.43, respectively). All HMs showed low contamination factor (CF < 1). The results of Pearson's correlation revealed high positive correlations between many elemental pairs (Table 3), such as between Fe and each of Co, Cu, Pb, Cr, As, Ni, V and Zn, suggesting natural sources for these HMs due to the presence of Fe, which is a well-defined marker for natural weathering and erosion of crustal materials (Mil-Homens et al., 2014; Mao et al., 2020). In the other hand, the weak correlations between Cu-As, Pb-As, and Pb-Cu may be indicated some contribution from other anthropogenic source for these HMs, such as municipal and domestic discharges (Tepe et al., 2022).

3.2. Human health risk assessment

Table 4 presented the results of the CDI, HQ and HI for non-carcinogenic risk of HMs from ingestion and dermal contact

Table 2
The minimum, maximum, and average values of the EF and CF.

	EF			CF		
	Min.	Max.	Aver.	Min.	Max.	Aver.
Pb	0.61	4.43	1.87	0.05	0.70	0.18
Zn	0.13	1.95	0.62	0.01	0.37	0.07
Cr	0.54	1.17	0.85	0.03	0.21	0.09
Ni	0.78	5.64	2.22	0.07	0.46	0.19
Cu	0.45	2.10	0.97	0.02	0.24	0.09
Fe				0.03	0.24	0.10
As	0.51	4.64	1.87	0.08	0.62	0.19
Co	0.32	1.18	0.75	0.01	0.09	0.03
V	0.19	0.91	0.48	0.02	0.15	0.05

Table 3
The correlation matrix of the analyzed HMs.

	As	Co	Cr	Cu	Fe	Ni	Pb	V	Zn
As	1								
Co	**.592****	1							
Cr	**.651****	**.912****	1						
Cu	.270	**.555****	**.524****	1					
Fe	**.559****	**.782****	**.925****	**.567****	1				
Ni	**.695****	**.862****	**.830****	.353*	**.599****	1			
Pb	.418*	**.687****	**.656****	.326	**.517****	**.662****	1		
V	**.694****	**.929****	**.976****	**.493****	**.843****	**.901****	**.653****	1	
Zn	**.566****	**.917****	**.892****	**.522****	**.742****	**.877****	**.847****	**.898****	1

**. Correlation is significant at the 0.01 level (2-tailed).
*. Correlation is significant at the 0.05 level (2-tailed).

Table 4
Chronic daily intake (CDI in mg/kg/day), hazard quotient (HQ) and cumulative hazard index (HI) for non-carcinogenic risk in adults and children.

HMs	**Adults**				
	CDI $_{Ing.}$	CDI $_{Dermal}$	HQ $_{Ing.}$	HQ $_{Demal}$	HI
As	3.223×10^{-6}	1.286×10^{-8}	1.074×10^{-2}	4.287×10^{-5}	1.079×10^{-2}
Cr	1.052×10^{-5}	4.196×10^{-8}	3.505×10^{-3}	1.399×10^{-5}	3.519×10^{-3}
Pb	4.472×10^{-6}	1.784×10^{-8}	1.278×10^{-3}	5.098×10^{-6}	1.283×10^{-3}
V	8.824×10^{-6}	3.521×10^{-8}	9.804×10^{-4}	3.912×10^{-6}	9.843×10^{-4}
Cu	5.520×10^{-6}	2.202×10^{-8}	1.488×10^{-4}	5.936×10^{-7}	1.494×10^{-4}
Ni	1.741×10^{-5}	6.945×10^{-8}	8.462×10^{-4}	3.472×10^{-6}	8.497×10^{-4}
Zn	8.542×10^{-6}	3.408×10^{-8}	2.847×10^{-5}	1.136×10^{-7}	2.859×10^{-5}
Co	1.894×10^{-6}	7.556×10^{-9}	9.468×10^{-5}	3.778×10^{-7}	9.506×10^{-5}
Fe	6.454×10^{-3}	2.575×10^{-5}	9.221×10^{-3}	3.679×10^{-5}	9.262×10^{-3}
HMs	**Children**				
	CDI $_{Ing.}$	CDI $_{Dermal}$	HQ $_{Ing.}$	HQ $_{Demal}$	Hi
As	3.008×10^{-5}	6.002×10^{-8}	1.003×10^{-1}	2.000×10^{-4}	1.005×10^{-1}
Cr	9.815×10^{-5}	1.958×10^{-7}	3.272×10^{-2}	1.958×10^{-7}	3.272×10^{-2}
Pb	4.174×10^{-5}	8.327×10^{-8}	1.193×10^{-2}	2.379×10^{-5}	1.195×10^{-2}
V	8.235×10^{-5}	1.643×10^{-7}	9.150×10^{-3}	1.825×10^{-5}	9.169×10^{-3}
Cu	5.152×10^{-5}	1.028×10^{-7}	1.389×10^{-3}	2.770×10^{-6}	1.391×10^{-3}
Ni	1.625×10^{-4}	3.241×10^{-7}	8.122×10^{-3}	1.620×10^{-5}	8.139×10^{-3}
Zn	7.972×10^{-5}	1.590×10^{-7}	2.657×10^{-4}	5.301×10^{-7}	2.663×10^{-4}
Co	1.767×10^{-5}	3.526×10^{-8}	8.837×10^{-4}	1.763×10^{-6}	8.855×10^{-4}
Fe	6.024×10^{-2}	1.202×10^{-4}	8.606×10^{-2}	1.717×10^{-4}	8.625×10^{-2}

Table 5
Carcinogenic risks for Cr, Pb, and As, and the total lifetime cancer risk (LCR) for adults and children via ingestion and dermal contact.

HMs	**Adults**			**Children**		
	CR $_{Ing.}$	CR $_{Dermal}$	LCR	CR $_{Ing.}$	CR $_{Dermal}$	LCR
As	4.835×10^{-6}	1.929×10^{-8}	4.85×10^{-6}	4.512×10^{-5}	9.002×10^{-8}	4.52×10^{-5}
Cr	5.258×10^{-6}	2.098×10^{-8}	5.28×10^{-6}	4.907×10^{-5}	9.790×10^{-8}	4.92×10^{-5}
Pb	3.801×10^{-8}	1.517×10^{-10}	3.82×10^{-8}	3.548×10^{-7}	7.078×10^{-10}	3.56×10^{-7}

pathways on adults and children. About adults, the maximum CDI values of the non-carcinogenic risk values were 6.454×10^{-3} mg/kg.day and 2.575×10^{-5} mg/kg. day through the ingestion and dermal pathways, respectively. In the other hand, the maximum CDI for children were 6.024×10^{-2} mg/kg. day and 1.202×10^{-4} mg/kg. day through the ingestion and dermal pathways, respectively. This difference indicated that children were at higher risk of non-carcinogenic exposure than adults.

The HI values varied from 2.859×10^{-5} to 1.079×10^{-2} for Adults, and from 2.663×10^{-4} to 1.005×10^{-1} for children. This means that the cumulative hazard index was higher among children compared to adults regarding the non-carcinogenic risk. However, our HI values for the HMs were less than 1.0, suggesting there is no significant non-carcinogenic risk to the people inhabiting the coastline of the Abu Ali Island (Tian et al., 2020). The HI values of HMs for both adults and children exhibited the following descending order: As > Fe > Cr > Pb > V > Ni > Cu > Co > Zn. However, the value of HI for As was greater than 0.1 for children, indicating the need to protect their health.

The accumulation of toxic HMs in human bodies may cause harmful complications. The excessive accumulation of Cr, As, and Pb in human bodies may trigger lung cancer, stomach cancer, dermal lesion, skin cancer, harmful to the respiratory system and can impact the nervous system and lead to renal failure (IARC, 1994; Mao et al., 2019; Rahman et al., 2021). The carcinogenic risks for Cr, Pb, and As were estimated in the studied samples (Table 5). About adults, the maximum carcinogenic risk values were 4.835×10^{-6} and 1.929×10^{-8} through the ingestion and dermal pathways, respectively. The maximum carcinogenic risk values for children were 4.512×10^{-5} and 9.002×10^{-8} through the ingestion and dermal pathways, respectively. The LCR values for adults ranged from 3.820×10^{-8} in Pb to 4.850×10^{-6} in As, and from 3.560×10^{-7} in Pb to 4.520×10^{-5} in As for children. LCR values revealed that no significant health hazards from the carcinogenic Pb, Cr, and As in the study area (Mondal et al., 2021), in spite of the risk in children is higher than that in adults due to their finger sucking behavior (Zhao et al., 2013; Pan et al., 2018).

4. Conclusions

This study highlighted HM contamination and human health risks along the Ras Abu Ali Island, Saudi Arabia. The averages of the HMs were in the order: Fe > Ni > Cr > Zn > V > Cu > Pb > As > Co. Ni, Pb, and As showed minor enrichment, while Fe, Cu, Co, Cr, Zn, and V determined no enrichment. Results of cumulative hazard index (HI) for non-carcinogenic risk of HMs and the carcinogenic risks for Cr, Pb, and As from ingestion and dermal contact pathways indicated no significant health hazards and the studied coastline is safe for vacationers, tourism, and the marine activities. Future studies will be needed to document the food chain uptake of contaminants and their human health implications along the Arabian Gulf.

Declaration of Competing Interest

The authors declare that they have no known competing financial interests or personal relationships that could have appeared to influence the work reported in this paper.

Acknowledgments

The authors extend their appreciation to Researchers Supporting Project number (RSP-2021/139), King Saud University, Riyadh, Saudi Arabia. Also, the authors would like to thank the anonymous reviewers for their valuable suggestions and constructive comments.

Appendix A. Supplementary material

Supplementary data to this article can be found online at https://doi.org/10.1016/j.jksus.2022.102509.

References

Alharbi, T., Alfaifi, H., Almadani, S.A., El-Sorogy, A., 2017. Spatial distribution and metal contamination in the coastal sediments of Al-Khafji area, Arabian Gulf, Saudi Arabia. Environ. Monit. Assess. 189, 634.

Al-Hashim, M.H., El-Sorogy, A.S., Al Qaisi, S., Alharbi, T., 2021. Contamination and ecological risk of heavy metals in Al-Uqair coastal sediments, Saudi Arabia. Mar. Pollut. Bull. 171, 112748.

Al-Kahtany, K.h., El-Sorogy, A.S., Al-Kahtany, F., Youssef, M., 2018. Heavy metals in mangrove sediments of the central Arabian Gulf shoreline, Saudi Arabia. Arab. J. Geosci. 11, 155.

Almahasheer, H., 2018. Spatial coverage of mangrove communities in the Arabian Gulf. Environ. Monit Assess., 19085

Bellas, J., Hylland, K., Burgeot, T., 2020. Editorial: New Challenges in Marine Pollution Monitoring. Front. Mar. Sci. 6, 820. https://doi.org/10.3389/fmars.2019.00820.

Demircan, H., El-Sorogy, A.S., Alharbi, T., 2021. Bioerosional structures from the Late Pleistocene coral reef, Red Sea coast, northwest Saudi Arabia. Turk. J. Earth Sci. 30, 22–37.

Di Cesare, A., Pjevac, P., Eckert, E., Curkov, N., Sparica, M.M., Corno, G., Orlic, S., 2020. The role of the metal contamination in shaping microbial communities in heavily polluted marine sediments. Environ. Pollut. 265,. https://doi.org/10.1016/j.envpol.2020.114823 114823.

El-Sorogy, A.S., 2015. Taphonomic processes of some intertidal gastropod and bivalve shells from northern Red Sea coast, Egypt. Pakistan J. Zool. 47 (5), 1287–1296.

El-Sorogy, A.S., Alharbi, T., Almadani, S., Al-Hashim, M., 2019. Molluscan assemblage as pollution indicators in Al-Khobar coastal plain, Arabian Gulf, Saudi Arabia. Journal of African Earth Sciences 158, 103564. https://doi.org/10.1016/j.jafrearsci.2019.103564.

El-Sorogy, A.S., Alharbi, T., Richiano, S., 2018b. Bioerosion structures in high-salinity marine environments: A case study from the Al–Khafji coastline, Saudi Arabia. Estuarine Coast. Shelf Sci. 204, 264–272.

El-Sorogy, A.S., Al-Kahtany, K., Youssef, M., Al-Kahtany, F., Al-Malky, M., 2018a. Distribution and metal contamination in the coastal sediments of Dammam Al-Jubail area, Arabian Gulf, Saudi Arabia. Mar. Pollut. Bull. 128, 8–16.

El-Sorogy, A.S., Attiah, A., 2015. Assessment of metal contamination in coastal sediments, seawaters and bivalves of the Mediterranean Sea coast, Egypt. Mar. Pollut. Bull. 101, 867–871.

El-Sorogy, A.S., Demircan, H., Alharbi, T., 2020. *Gastrochaenolites* ichnofacies from intertidal seashells, Al-Khobar coastline, Saudi Arabia. J. Afr. Earth Sc. 171 http://www.ncbi.nlm.nih.gov/pubmed/103943.

El-Sorogy, A.S., Demircan, H., Al-Kahtany, K.h., 2021. Taphonomic signatures on modern molluscs and corals from Red Sea coast, southern Saudi Arabia. Palaeoworld. https://doi.org/10.1016/j.palwor.2021.07.001.

El-Sorogy, A.S., Tawfik, M., Almadani, S.A., Attiah, A., 2016. Assessment of toxic metals in coastal sediments of the Rosetta area, Mediterranean Sea, Egypt. Environ. Earth Sci. 75, 398.

El-Sorogy, A.S., Youssef, M., 2015. Assessment of heavy metal contamination in intertidal gastropod and bivalve shells from central Arabian Gulf coastline, Saudi Arabia. J. Afr. Earth Sci. 111, 41–53.

Hakanson, L., 1980. An ecological risk index for aquatic pollution control. A sedimentological approach. Water Res. 14, 975–1001.

IARC, 1994. Monographs on the evaluation of carcinogenic risks to humans. Some Ind. Chem. 60, 389–433.

IRIS, Program Database 2020. Available online: https://cfpub.epa.gov/ncea/iris/search/index.cfm (accessed on 18 September 2020).

Kahal, A., El-Sorogy, A.S., Qaysi, S., Almadani, S., Kassem, O.M., Al-Dossari, A., 2020. Contamination and ecological risk assessment of the Red Sea coastal sediments, southwest Saudi Arabia. Mar. Pollut. Bull. 154, 111125.

Kowalska, J.B., Mazurek, R., Gasiorek, M., Zaleski, T., 2018. Pollution indices as useful tools for the comprehensive evaluation of the degree of soil contamination–A review. Environ. Geochem. Health 40, 2395–2420.

Luo, X.S., Ding, J., Xu, B., Wang, Y.J., Li, H.B., Yu, S., 2012. Incorporating bioaccessibility into human health risk assessments of heavy metals in urban park soils. Sci. Total Environ. 424, 88–96.

Ma, J., Pan, L.B., Wang, Q., Lin, C.Y., Duan, X.L., Hou, H., 2016. Estimation of the daily soil/dust (SD) ingestion rate of children from Gansu Province, China via hand-to-mouth contact using tracer elements. Environ. Geochem. Health. https://doi.org/10.1007/s10653-016-9906-1.

Mao, C., Song, Y., Chen, L., Ji, J., Li, J., Yuan, X., Yang, Z., Ayoko, G.A., Frost, R.L., Theiss, F., 2019. Human health risks of heavy metals in paddy rice based on transfer characteristics of heavy metals from soil to rice. Catena 175, 339–348.

Mao, L., Liu, L., Yan, N., Li, F., Tao, H., Ye, H., Wen, H., 2020. Factors controlling the accumulation and ecological risk of trace metal(loid)s in river sediments in agricultural field. Chemosphere 243, 125359.

Mil-Homens, M., Vale, C., Raimundo, J., Pereira, P., Brito, P., Caetano, M., 2014. Major factors influencing the elemental composition of surface estuarine sediments: the case of 15 estuaries in Portugal. Mar. Pollut. Bull. 84, 135–146.

Mondal, P., Lofrano, G., Carotenuto, M., Guida, M., Trifuoggi, M., Libralato, G., Sarkar, S.K., 2021. Health Risk and Geochemical Assessment of Trace Elements in Surface Sediment along the Hooghly (Ganges) River Estuary (India). Water 13, 110. https://doi.org/10.3390/w13020110.

Naveedullah Hashmi, M.Z., Yu, C., Shen, H., Duan, D., Shen, C., Lou, L., Chen, Y., 2014. Concentrations and Human Health Risk Assessment of Selected Heavy Metals in Surface Water of the Siling Reservoir Watershed in Zhejiang Province, China. Pol. J. Environ. Stud. 23 (3), 801–811.

Nazzal, Y., Orm, N.B., Barbulescu, A., Howari, F., Sharma, M., Badawi, A.E., Al-Taani, A., Iqbal, J., Ktaibi, F.E., Xavier, C.M., et al., 2021, Study of atmospheric pollution and health risk assessment: A case study for the Sharjah and Ajman Emirates (UAE). Atmosphere 12, 1442. https://doi.org/10.3390/atmos12111442.

Nour, H.N., Alshehri, F., Sahour, H., El-Sorogy, A.S., Tawfik, M., 2022. Assessment of heavy metal contamination and health risk in the coastal sediments of Suez Bay, Gulf of Suez, Egypt. J. African Earth Sci. 195,. https://doi.org/10.1016/j.jafrearsci.2022.104663 104663.

Pan, L., Wang, Y., Ma, J., Hu, Y., Su, B., Fang, G., Wang, L., Xiang, B., 2018. A review of heavy metal pollution levels and health risk assessment of urban soils in Chinese cities. Environ. Sci. Pollut. Res. 25, 1055–1069. https://doi.org/10.1007/s11356-017-0513-1.

Rahman, M.S., Kumar, P., Ullah, M., Jolly, Y.N., Akhter, S., Kabir, J., Begum, B.A., Salam, A., 2021. Elemental analysis in surface soil and dust of roadside academic institutions in Dhaka city, Bangladesh and their impact on human health. Environ. Chem. Ecotoxicol. 3, 197–208.

Rajeshkumar, S., Liu, Y., Zhang, X., Ravikumar, B., Bai, G., Li, X., 2018. Studies on seasonal pollution of metals in water, sediment, fish and oyster from the Meiliang Bay of Taihu Lake in China. Chemosphere 191, 626–638.

Reimann, C., de Caritat, P., 2005. Distinguishing between natural and anthropogenic sources for elements in the environment: Regional geochemical surveys versus enrichment factors. Sci. Total Environ. 337, 91–107.

Rudnick, R.L., Gao, S., 2003. Composition of the continental crust. Treatise Geochem. 3, 1–64. https://doi.org/10.1016/B0-08-043751-6/03016-4.

Saavedra, J.V., Quiroga, E., 2021. Risk assessment for marine sediment associated metals and metalloid using multiple background reference values and environmental indexes. The case of the Concon-Quintero industrial complex, Central Chile. Marine Pollution Bulletin (Accepted).

Saderne, V., Cusack, M., Serrano, O., Almahasheer, H., Krishnakumar, P.K., Rabaoui, L., Qurban, M.A., Duarte, C.M., 2020. Role of vegetated coastal ecosystems as nitrogen and phosphorous filters and sinks in the coasts of Saudi Arabia. Environ. Res. Lett. 15,. https://doi.org/10.1088/1748-9326/ab76da 034058.

Simpson, S.L., Batley, G.B., Chariton, A.A., 2013. Revision of the ANZECC/ARMCANZ Sediment Quality Guidelines. CSIRO Land and Water Science Report 08/07. CSIRO Land and Water, 119–p.

Singovszka, E., Balintova, M., Demcak, S., Pavlikova, P., 2017. Metal pollution indices of bottom sediment and surface water affected by acid mine drainage. Metals 7, 284.

Song, Q., Li, J., 2014. A review on human health consequences of metals exposure to, e-waste in China. Environ. Pollut. 196C, 450–461.

Taylor, S.R., 1964. Abundance of chemical elements in the continental crust: a new table. Geoch. Cosmoch. Acta 28, 1273–1285. https://doi.org/10.1016/0016-7037(64)90129-2.

Tepe, Y., Şimşek, A., Ustaoğlu, F., et al., 2022. Spatial–temporal distribution and pollution indices of heavy metals in the Turnasuyu Stream sediment, Turkey. Environ. Monit. Assess. 194, 818. https://doi.org/10.1007/s10661-022-10490-1.

Tian, S., Wang, S., Bai, X., Zhou, D., Luo, G., Yang, Y., Hu, Z., Li, C., Deng, Y., Lu, Q., 2020. Ecological security and health risk assessment of soil heavy metals on a village-level scale, based on different land use types. Environ. Geochem. Health 42, 3393–3413. https://doi.org/10.1007/s10653-020-00583-6.

Tonne, C., Adair, L., Adlakha, D., Anguelovski, I., Belesova, K., Berger, M., Brelsford, C., Dadvand, P., Dimitrova, A., Giles-Corti, B., Heinz, A., Mehran, N., Nieuwenhuijsen, M., Pelletier, F., Ranzani, O., Rodenstein, M., Rybski, D., Samavati, S., Satterthwaite, D., Schöndorf, J., Schreckenberg, D., Stollmann, J., Taubenböck, H., Tiwari, G., van Wee, B., Adli, M., 2021. Defining pathways to healthy sustainable urban development. Environ. Int. 146,. https://doi.org/10.1016/j.envint.2020.106236 106236.

Turekian, K.K., Wedepohl, K.H., 1961. Distribution of the elements in some major units of the earth's crust. Geol. Soc. Amer. 72, 175–192. https://doi.org/10.1130/0016-7606(1961)72[175:DOTEIS]2.0.CO;2.

Ustaoğlu, F., Tepe, Y., 2019. Water quality and sediment contamination assessment of Pazarsuyu Stream, Turkey using multivariate statistical methods and pollution indicators. Int. Soil Water Conserv. Res. 7, 47–56. https://doi.org/10.1016/j.iswcr.2018.09.001.

Ustaoğlu, F., Tepe, Y., Aydin, H., 2020. Heavy metals in sediments of two nearby streams from Southeastern Black Sea coast: Contamination and ecological risk assessment. Environ. Forensic 21 (2), 145–156. https://doi.org/10.1080/15275922.2020.1728433.

Wu, B., Wang, G., Wu, J., Fu, Q., Liu, C., 2014. Sources of metals in surface sediments and an ecological risk assessment from two adjacent plateau reservoirs. PLoS One 9, 1–14.

Yaroshevsky, A.A., 2006. Abundances of chemical elements in the Earth's crust. Geochem. Internat. 44 (1), 48–55. https://doi.org/10.1134/S001670290601006X.

Zhao, L., Xu, Y., Hou, H., Shangguan, Y., Li, F. 2013. Source identification and health risk assessment of metals in urban soils around the Tanggu chemical industrial district, Tianjin, China. Sci. The Total Environ. 468-469C, 654–662.